Morphology and Deformation Mechanism of Segmented Poly(urethaneureas) in Relation to Spherulitic Crystalline Textures[1a]

Itsuro Kimura,[1b] Hideaki Ishihara,[1b] Hiroshi Ono,[1b] Nori Yoshihara,[1c] Shunji Nomura,[1c] and Hiromichi Kawai*,[1c]

Katata Research Institute, Toyo-bo Co., Ltd., Katata, Shiga-ken, Japan, and the Department of Polymer Chemistry, Faculty of Engineering, Kyoto University, Kyoto, Japan.
Received October 4, 1973

ABSTRACT: A new finding on the spherulitic crystalline texture of a particular type of segmented poly(urethaneureas) was demonstrated by polarized small-angle light scattering. The polymers were synthesized by coupling a prepolymer consisting of poly(tetramethylene glycol) (PTMG) and 4,4′-diphenylmethane diisocyanate (DMI) with four kinds of chain extenders, ethylenediamine (EDA), propylenediamine (PDA), hydrazine (HH), and diaminodiphenylmethane (DAM). The deformation mechanism of the spherulitic crystalline texture and its disintegration into a paracrystalline fiber texture were investigated by means of infrared dichroism, wide-angle X-ray diffraction, small-angle X-ray scattering, and polarized small-angle light scattering. The results are discussed in terms of the deformation parameters of a model of spherulite deformation proposed by some of the present authors.

In 1963, Sadron demonstrated micelle formation in an A–B-type block copolymer of styrene and ethylene oxide due to microphase separation of the block segments at the critical micelle concentration.[2a] Since then, the mechanism of domain formation, during casting of block and graft copolymers from their solutions into solid specimens, has been extensively studied by many authors, mostly for A–B- and A–B–A-type block copolymers.[2b,3]

Segmented polymers, on the other hand, have not been fully studied with regard to the microphase separation of the block segments, because of their complicated sequence arrangements.[4-6] Segmented poly(urethanes), especially segmented poly(urethaneureas) described in this paper, were considered as simple alternating copolymers of a single urea group and the so-called soft segment. It has been shown, however, that most of the segmented poly(urethanes) exhibit some blockiness in the sequence of the so-called hard segments.[7] This suggests that the segmented poly(urethanes) can be classified as an intermediate system between an alternating copolymer and a really multiblock copolymer, the position in the classification depending on the composition and preparation method of the materials.

In this paper, a new aspect of the spherulitic crystalline texture of particular types of segmented poly(urethaneureas) and their mechanisms of deformation and disintegration into a paracrystalline fiber texture, will be demonstrated in terms of polarized small-angle light-scattering patterns. The results will be discussed in terms of a model of spherulite deformation describing the orientation behavior of the hard and soft segments of these copolymers measured by infrared dichroism and small- and wide-angle X-ray diffractions.[8,9]

The results will be useful not only for discussing the paracrystalline fiber texture in the ultimate stage of highly stretched specimens,[6,10] but also for understanding the elasticity of the segmented poly(urethanes) in terms of orientation and deformation mechanisms of molecular and supermolecular structures. In addition, this report describes the similarities and dissimilarities between segmented poly(urethanes) and multiblock copolymers in terms of the effect of sequence arrangements as well as crystalline and noncrystalline characteristics of the block segments on the domain formation mechanism.[11-14]

Test Specimens. Four types of segmented poly(urethaneureas) were synthesized by coupling a prepolymer consisting of poly(tetramethylene glycol) (PTMG) and 4,4′-diphenylmethane diisocyanate (DMI), with four kinds of chain extenders, ethylenediamine (EDA), propylenediamine (PDA), hydrazine (HH), and diaminodiphenylmethane (DAM), so that these segmented poly(urethaneureas) consist of a chain of poly(tetramethylene oxide) linked by urethane groups and a sequence of urea groups. The molar ratio of PTMG to diisocyanate in the prepolymer reaction was taken as 2.

The soft segment and the four kinds of hard segments are given, respectively, in Chart I, where l, m, and n are averages of sequence distributions of the units which depend on the polymerization condition. In this study, l varies from about 10 to 30, while m and, subsequently, n, which also depend on the polymerization condition of the prepolymer, are estimated to be about 5.[7] The nomenclature of the poly(urethaneureas) will be illustrated using the example of PTMG(1000)–DMI:HH. In accordance with the above molecular structures, PTMG(1000)–DMI designates the prepolymer consisting of poly(tetramethylene glycol) having a molecular weight of about 1000, attached to 4,4′-diphenylmethane diisocyanate DMI, and HH means an (HH)-type chain extender. These copolymers were cast into thin films of from several to several tens of microns in thickness by pouring about 10% solutions in dimethylacetamide on glass plates at about 70°.

Experimental Results and Discussions

Infrared Dichroism. The orientation behavior of the hard and soft segments during stretching of the film specimens was represented in terms of an uniaxial orientation factor of the transition moments of particular groups. The orientation factor is defined by[15]

$$F^D = (3\langle\cos^2\theta\rangle - 1)/2 = (A_\parallel - A_\perp)/(A_\parallel + 2A_\perp) \quad (1)$$

where θ is the orientation angle of the transition moment with respect to the stretching direction, and $A_\parallel$ and $A_\perp$ are absorption coefficients of polarized light parallel and perpendicular to the stretching direction of the specimen, respectively.

The orientation behavior of the hard segments is illustrated in Figures 1-3 in terms of the change of the orientation factor of the transition moment of the ν(C=O), amide I absorption of the urea group with % elongation of the film specimens. This absorption occurs at 1640 cm^{-1} for EDA, PDA, and DAM and at 1680 cm^{-1} for HH.[8] As

Chart I

Soft segment

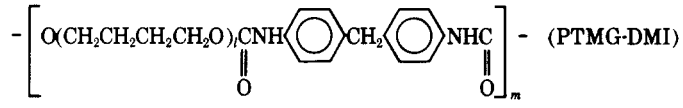

Hard segments

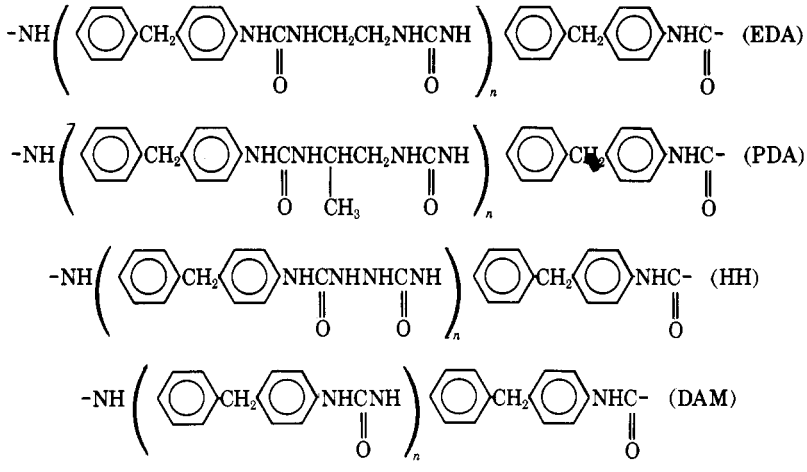

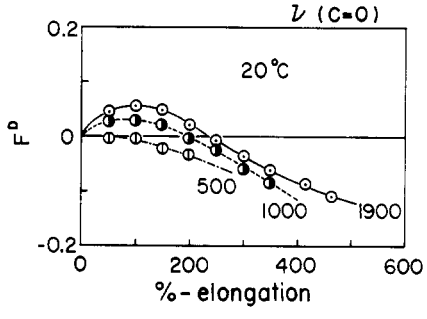

Figure 1. Orientation behavior of the hard segment in terms of the change of orientation factor of the transition moment of ν(C=O), amide I absorption of urea group, with % elongation of a series of specimens having a particular type of hard segment (HH) with a different length of soft segment (PTMG-DMI).

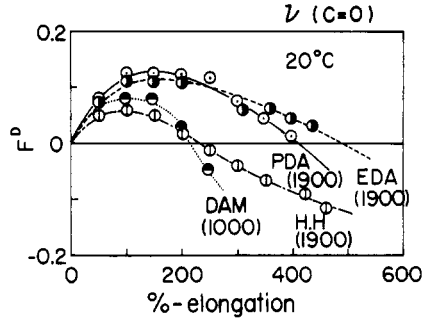

Figure 2. Orientation behavior of the hard segment in terms of the change of orientation factor of the transition moment of ν(C=O), amide I absorption of urea group, with % elongation of a series of specimens having different types of hard segment with a given length of soft segment.

seen in the figures, the orientation behavior of the transition moment of the ν(C=O) gives, in general, positive orientation at relatively small % elongations, but changes to negative orientation with further increase of the % elongation. Shorter soft segments and higher stretching temperatures shift this transition from positive to negative orientations to smaller % elongations. Actually, as seen in Figure 3 for PTMG(1900)-DMI:PDA at 75-80°, the positive orientation diminishes significantly and the negative orientation appears from the beginning of the stretching. This type of shift is also related to the molecular structures of the hard segments, as seen definitely in Figure 2 for the (HH) segment. This shift is probably due to the imperfection of crystalline superstructure formed by the hard segments, and will be discussed later. In addition, Figure 3 also shows that for the cyclic deformations, when the recovery cycle is performed from relatively small % elongations, the orientation recovers from positive to zero or slightly negative, but when the recovery cycle is started from relatively large % elongations, the orientation does not recover to zero but remains negative or even goes further negative.

The transition moment of the ν(C=O) may be assumed to orient perpendicular to the chain direction. If this is the case, then the above orientation behavior suggests, in general, the negative orientation of the hard segments at relatively small % elongations and the transition to positive orientation with further increase of the % elongation. This transition can be shifted, as mentioned above, by the stretching condition as well as by the combination of molecular structures of the soft and hard segments.

The orientation behavior of the soft segments is illustrated in Figures 4 and 5 in terms of the $\omega(CH_2)$ and $\nu_a(CH_2)_{II}$, wagging and anti-symmetric stretching vibrations of CH_2 group, with % elongation of the film specimens. These vibrations have wave numbers of 1370 and 2940 cm^{-1}, respectively. As seen in the figures, the orientation behavior of the transition moments of the $\omega(CH_2)$ and $\nu_a(CH_2)_{II}$ gives monotonous increases of positive and negative orientations, respectively. The transition moments of the $\omega(CH_2)$ and $\nu_a(CH_2)_{II}$ may be assumed to orient parallel and perpendicular to the chain direction, respectively, and this contrasting behavior can be simply understood as a monotonous increase of positive orientation of the soft segments with stretching of the film specimens.

Small- and Wide-Angle X-Ray Diffraction. Bonart has investigated the paracrystalline structure of segmented poly(urethaneureas) consisting of the (HH)- and (EDA)-type hard segments.[6] Unfortunately, in his study of the paracrystalline nature of the materials, his attention was mostly attracted to the diatropic reflections, missing the paratropic ones. In the present study, the crystal orientation behavior of the four types of segmented

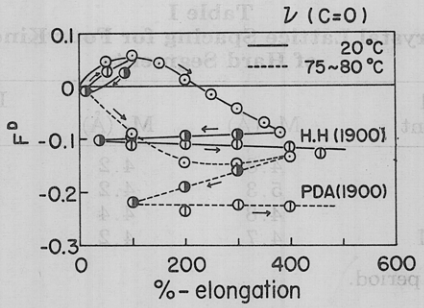

Figure 3. Orientation behavior of the hard segment in terms of the change of orientation factor of the transition moment of ν(C=O), amide I absorption of urea group, with cyclic deformation of two kinds of specimens at two different temperatures.

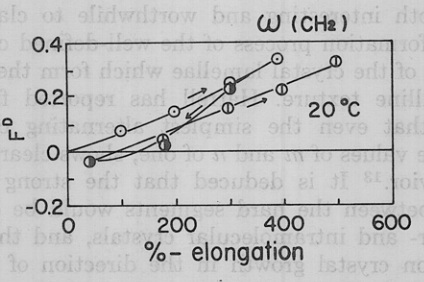

Figure 4. Orientation behavior of the soft segment in terms of the change of orientation factor of the transition moment of $\omega(CH_2)$, wagging vibration of CH_2 group, with % elongation of specimen, PTMG(1900)–DMI:HH.

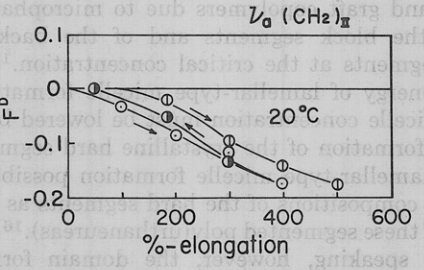

Figure 5. Orientation behavior of the soft segment in terms of the change of orientation factor of the transition moment of $\nu_a(CH_2)_{II}$, anti-symmetric stretching vibration of CH_2 group, with % elongation of specimen, PTMG(1900)–DMI:HH.

poly(urethaneureas) is demonstrated in terms of the changes of the intensity distribution of X-ray diffraction, not only from the diatropic crystal planes but also from the paratropic ones, all with stretching of the film specimens.

Figure 6 shows, for example, the changes of the wide-angle X-ray diffraction pattern of a film specimen of PTMG(500)–DMI:PDA with stretching at room temperature and also with heat treatment of 180° for 1 min in a highly stretched state of the specimen. The crystalline diffractions indicated by M_1 and M_2 in the figure, are assigned to paratropic reflections from the highly stretched pattern. On the other hand, a crystalline diffraction with a much smaller Bragg angle than the M_1 and M_2 diffractions must be assigned to diatropic reflection. This diffraction is hardly seen for the unstretched or slightly stretched pattern, but is definitely seen for the highly stretched and heat-treated pattern with higher order reflections up to sixth order in the meridional direction clearly visible. All of these crystalline diffractions must arise from crystallites composed of the hard segments, simply because these crystalline diffractions do not disappear at temperatures higher than the melting point of PTMG (soft segment) found at around 50°. Furthermore, the crystalline diffractions from PTMG, which are found, as demonstrated in Figure 7 for PTMG(1900)–DMI:EDA,

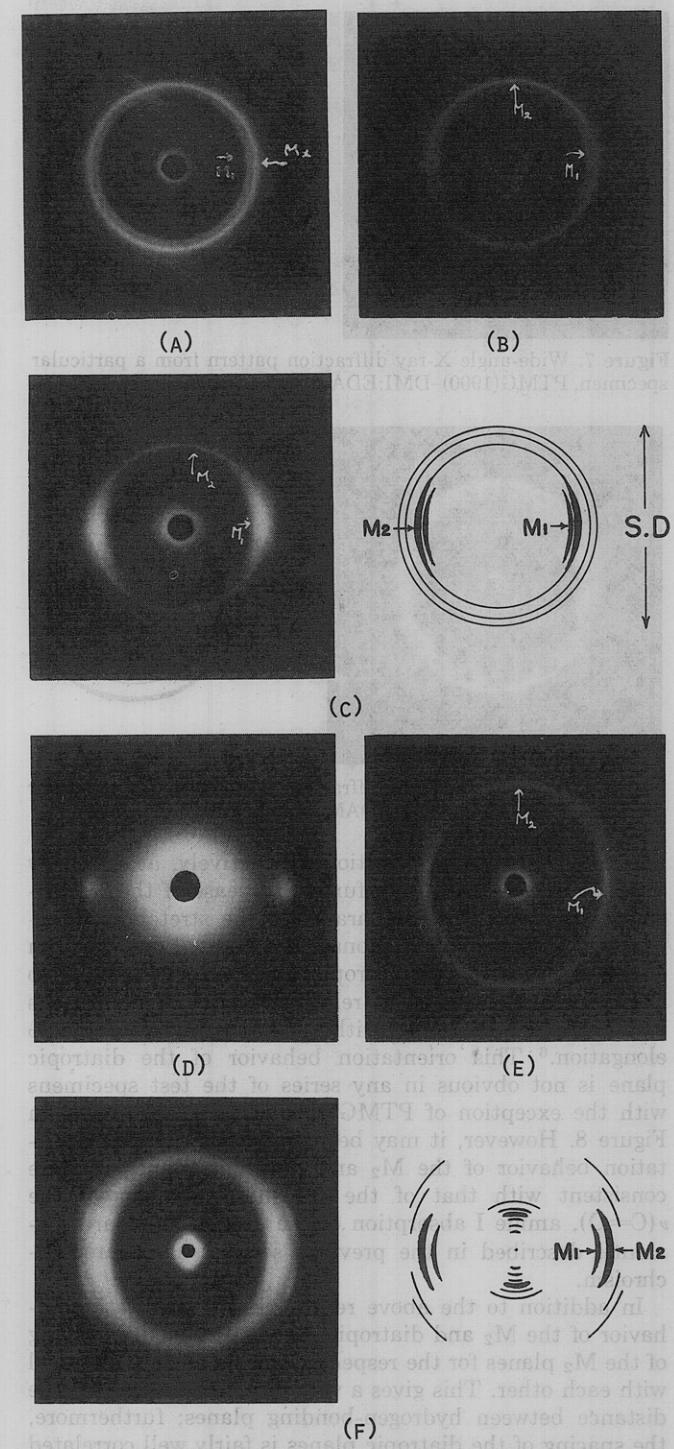

Figure 6. Changes of wide-angle X-ray diffraction pattern of a particular specimen PTMG(500)–DMI:PDA with stretching at room temperature and with a heat treatment at 180° for 1 min in a highly stretched state: (A) unstretched, (B) stretched by 100% elongation, (C) stretched by 300% elongation, (D) stretched by 500% elongation, (E) edge radiation pattern from rolled specimen, and (F) stretched by 600% elongation and heat treated at 180° for 1 min.

at room temperature only for highly stretched specimen, appear in the equatorial zone, with a spacing different from those of M_1 and M_2. The lattice spacing of these paratropic and diatropic crystal planes of the hard segment crystals are listed in Table I. The values of the diatropic planes are evaluated from the most intensive reflections, except for PDA for which the value of 50 Å can be considered as the fiber identical period.

As seen in Figure 6, the M_1 and M_2 planes orient in opposite directions from each other, parallel and perpendic-

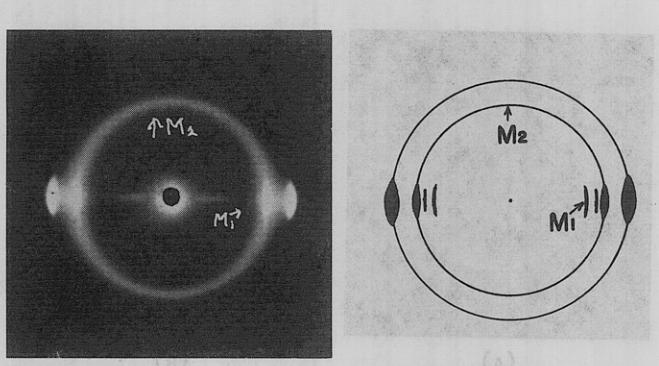

Figure 7. Wide-angle X-ray diffraction pattern from a particular specimen, PTMG(1900)–DMI:EDA stretched 300% elongation.

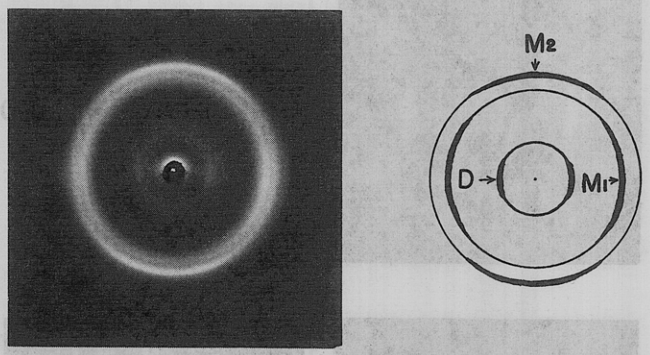

Figure 8. Wide-angle X-ray diffraction pattern from a particular specimen, PTMG(1000)–DMI:DAM stretched 100% elongation.

ular to the stretching direction, respectively, at relatively small % elongations. With further increase of the % elongation, they both orient parallel to the stretching direction. On the other hand, Bonart has pointed out, from an X-ray study, that the diatropic plane orients parallel to the stretching direction at relatively small % elongations and turns perpendicular with further increase of the % elongation.[6] This orientation behavior of the diatropic plane is not obvious in any series of the test specimens with the exception of PTMG(1000)–DMI:DAM shown in Figure 8. However, it may be pointed out that the orientation behavior of the M_2 and diatropic planes is quite consistent with that of the transition moment of the ν(C=O), amide I absorption of the urea group (hard segment), described in the previous section on infrared dichroism.

In addition to the above results on the orientation behavior of the M_2 and diatropic planes, the lattice spacing of the M_2 planes for the respective specimens are identical with each other. This gives a very reasonable value for the distance between hydrogen-bonding planes; furthermore, the spacing of the diatropic planes is fairly well correlated with the repeating structure of the hard segments. These facts suggest strongly that the reciprocal lattice vectors of the M_2 and diatropic planes orient orthogonally to each other and parallel to the directions of the hydrogen bonding between the hard segments and of the chain contour of the hard segment, respectively. The direction of the reciprocal lattice vector of the M_1 plane must be perpendicular to the plane including the two reciprocal lattice vectors of the M_2 and diatropic planes. This is suggested from the above-mentioned orientation behavior and is demonstrated in Figure 6 in terms of the double orientation picture of X-ray diffraction for a rolled specimen. Figure 9 shows the dependence of the long period on the molecular weight of the soft segment, observed from small-angle X-ray scattering from a series of highly stretched, heat-treated, and relaxed PTMG–DMI:PDA. When extrapolated to zero molecular weight of the

Table I
Crystal Lattice Spacing for Four Kinds of Hard Segments

Hard Segment	M_1 (Å)	M_2 (Å)	Diatrop (A)
HH	4.8	4.2	12
EDA	5.3	4.2	13.5
PDA	4.8	4.4	50[a]
DAM	4.7	4.2	11.5

[a] Fiber period.

PTMG, the value of the long period of around 85 Å will give the lamellar thickness, which is consistent with the fully extended length of PDA having the value of n around 5.

It is both interesting and worthwhile to clarify more fully the formation process of the well-defined crystallites as well as of the crystal lamellae which form the spherulitic crystalline texture. Harrell has reported from DSC analysis that even the simplest alternating copolymer, having the values of m and n of one, shows clear-cut melting behavior.[13] It is deduced that the strong hydrogen bonding between the hard segments would be enough to form inter- and intramolecular crystals, and that the restriction on crystal growth in the direction of the chain axis, which is due to its alternating structure with soft segments, would greatly favor the formation of crystal lamellae. It may also be interesting to understand the lamellar formation from the view point of micelle formation of block and graft copolymers due to microphase separations of the block segments and of the backbone and grafted segments at the critical concentration.[11,12] Thus, the free energy of lamellar-type micelle formation at the critical micelle concentration must be lowered by the stiff chain conformation of the crystalline hard segments so as to make lamellar-type micelle formation possible even at fractional compositions of the hard segments as low as *ca.* 20 wt % of these segmented poly(urthaneureas).[16]

Strictly speaking, however, the domain formation of block copolymers of crystalline and noncrystalline segments from their solutions must be discussed in relation to both the critical micelle concentration for microphase separation of the block segments and the critical crystallization concentration of the crystalline block segments, *i.e.,* which of these two is proceeding during the casting process of the system for a given solvent at a given temperature. Actually, as will be demonstrated elsewhere,[17] for particular systems of A–B- and A–B–A-type block copolymers of ethylene oxide and isoprene in benzene and ethylbenzene, the lamellar formation and, subsequently, spherulite formation depends not only the fractional composition of the block sequences, but also greatly on the nature of the solvent.

The above-mentioned orientation behavior of the three crystallographic axes as well as of the amorphous soft segments, especially the transition phenomena of crystal orientation behavior, may be explained in terms of two different orientation mechanisms in association with deformation and disintegration of the crystalline texture. This is illustrated schematically in Figure 10 for a part of the spherulitic texture and its deformation. At relatively small % elongations, the crystalline lamellae would be taken as orientation units floating in a matrix of the soft segments. In these units, the lamellar axis (reciprocal lattice vector of the M_2 plane) should be the principal orientation axis which gives its positive orientation around which the other two crystallographic axes orient randomly to give equal negative orientations. At relatively large % elongations, on the other hand, the oriented lamellae

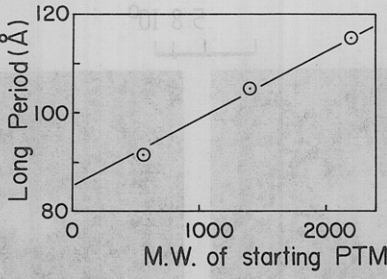

Figure 9. Dependence of the long period on the molecular weight of soft segment, obtained from small-angle X-ray scattering from a series of highly stretched, heat-treated and relaxed specimens of PTMG–DMI:PDA.

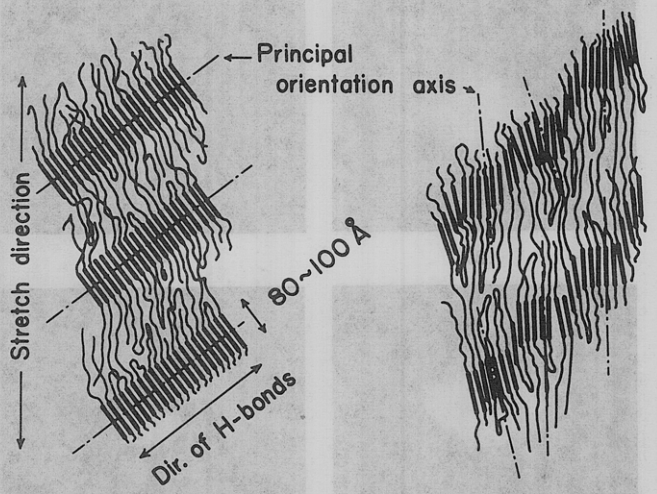

Figure 10. Schematic diagrams illustrating a part of spherulitic texture (left-hand side) and its deformation and disintegration mechanisms with stretching (right-hand side) of the segmented poly(urethaneureas), where thick and thin lines indicate the hard and soft segments, respectively.

would disintegrate into small fragments to give diffuse X-ray diffraction, as seen in Figure 6 for 500 % elongation. Here the hard segment axis turns out to be the principal orientation axis giving its positive orientation around which the two reciprocal lattice vectors of the M_1 and M_2 planes orient randomly to give their negative orientations. The amorphous soft segments, which compose the matrix and act as the so-called tie chains between the lamellae, give more or less positive orientation irrespective of the transition of the crystal orientation behavior. Shorter soft segments and higher stretching temperatures lead to smaller % elongations at which the disintegration of the crystal lamella and the transition of the crystal orientation occur.

Small-Angle Polarized Light Scattering. Figure 11 shows the cross- and parallel-polarized (the so-called H_v and V_v) light-scattering patterns from the film specimens of the four kinds of segmented poly(urethaneureas). As can be recognized from the patterns, the specimens have definitely symmetric-crystalline textures, changing from an almost perfect spherulitic texture to a truncated spherulitic texture[18,19] and probably to a texture of a random assembly of anisotropic rods[20,21] in the order of DAM, PDA, EDA, and HH. In all these the spherulitic textures may be classified as the so-called negative spherulite, providing that α_s is slightly larger than α_r.[22,23] The size of the spherulitic textures changes also in the same order as the above from a radius of about 10 μ for PTMG(1000)–DMI:DAM to about 3 μ for PTMG(500)–DMI:HH. Figure 12 illustrates the extremes of the cross-polarized micrographs obtained from the film specimens of PTMG(1000)–DMI:DAM and PTMG(500)–DMI:HH,

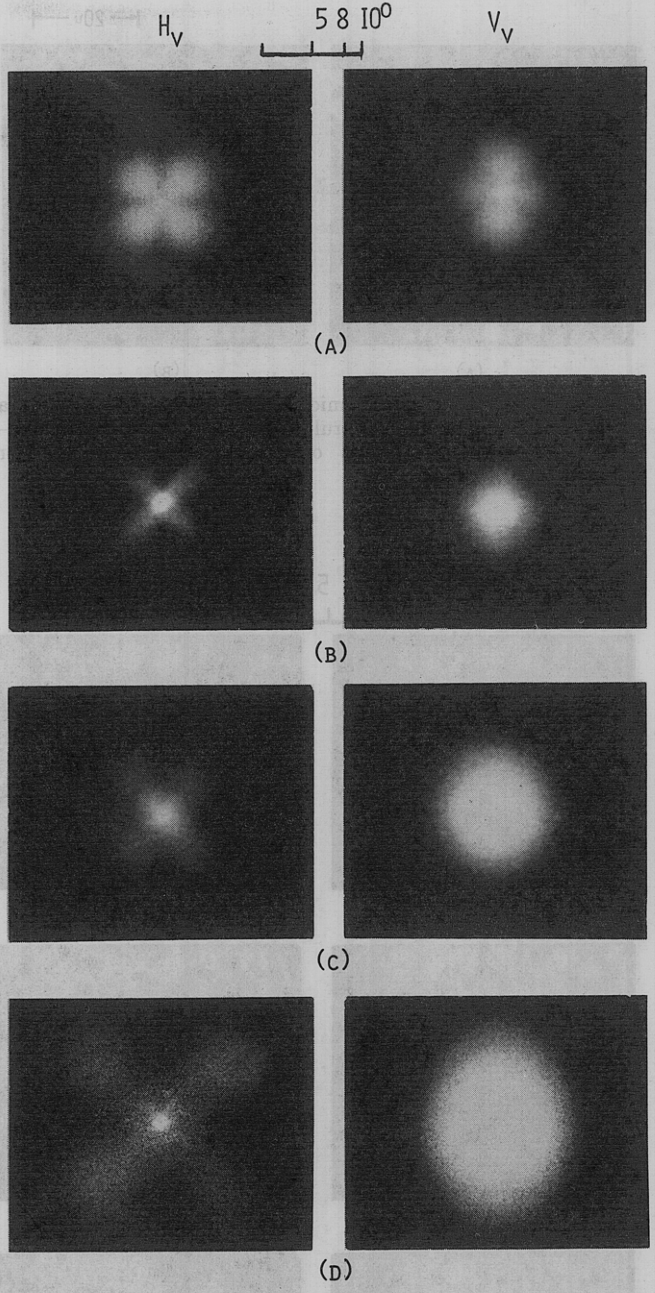

Figure 11. H_v and V_v light-scattering patterns from a series of specimens having different types of hard segments: (A) PTMG(1000)–DMI:DAM, (B) PTMG(500)–DMI:PDA, (C) PTMG(500)–DMI:EDA, and (D) PTMG(500)–DMI:HH.

justifying the above explanations of the crystalline textures in terms of a well-defined spherulitic crystalline texture and a less ordered one, respectively.

Figures 13 and 14 show the changes of H_v and V_v light-scattering patterns of PTMG(1000)–DMI:DAM with stretching and relaxation at room temperature and with a heat treatment, respectively. The heat treatment was performed by fixing the specimen with 500% elongation at 180° for 1 min. As can be seen in the figures, the change of the pattern with stretching is typical of the behavior obtained experimentally and theoretically from a uniaxially deformed spherulitic crystalline texture, such as deformed polyethylene and polypropylene spheluties.[24,25] However, at around 500% elongation, a vertical streak appears both for the H_v and V_v patterns; also, a pair of streaks can be seen somewhat inclined to the horizontal direction in highly stretched states for the V_v patterns. The vertical streak may be ascribed to the development of microvoids

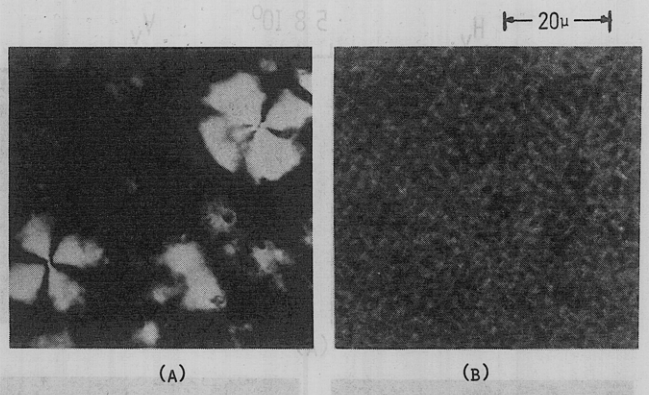

Figure 12. Cross-polarized micrographs demonstrating (A) a well-defined crystalline spherulitic texture for PTMG(1000)–DMI:DAM and (B) a less ordered crystalline texture for PTMG(500)–DMI:HH.

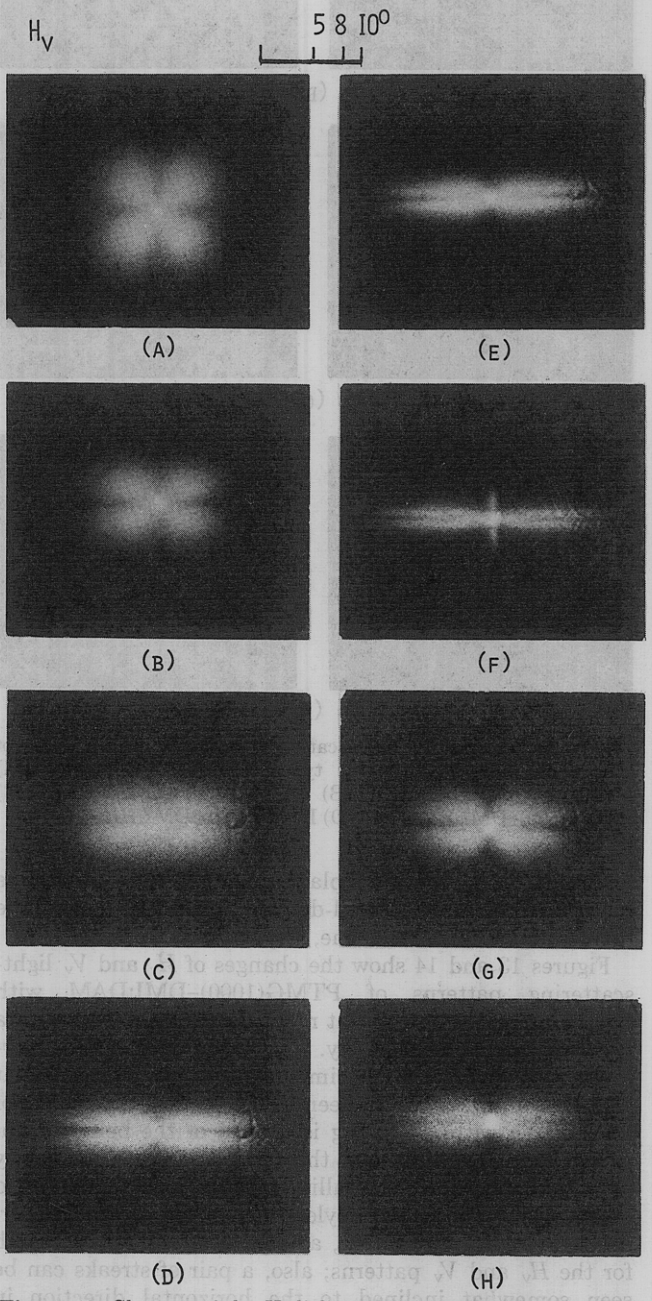

Figure 13. Changes of the H_v light-scattering pattern from a particular specimen PTMG(1000)–DMI:DAM with stretching, relaxing, and heat treatment in a highly stretched state.

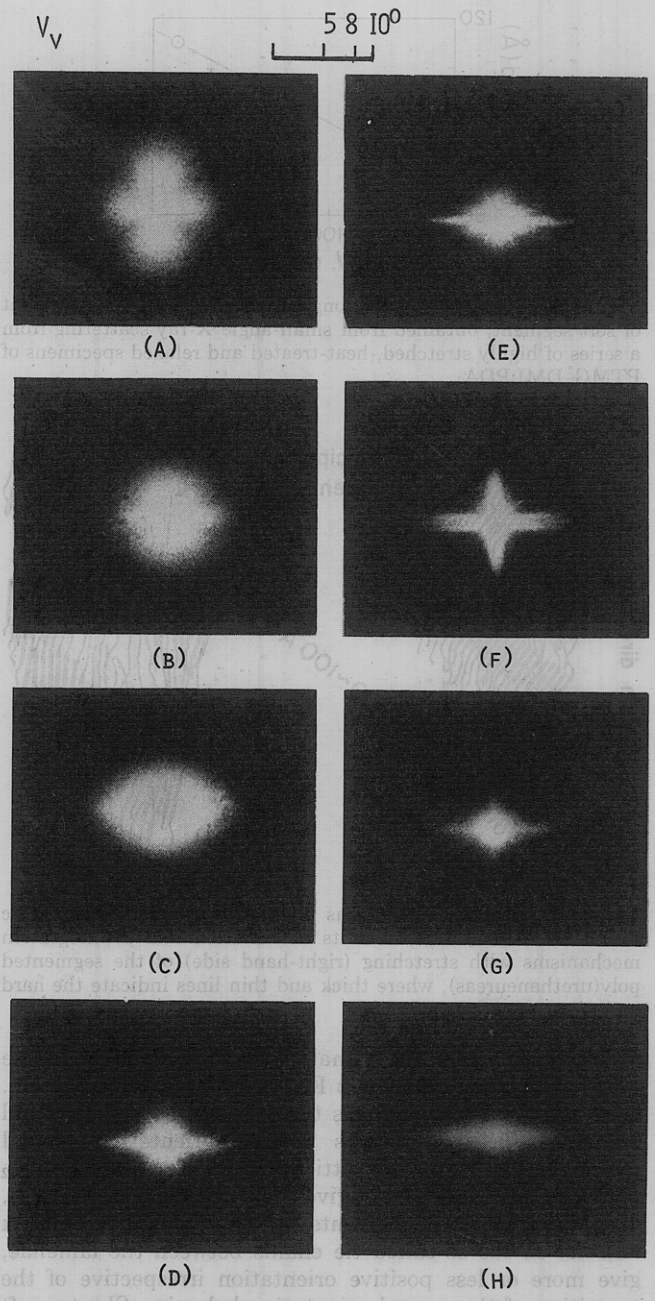

Figure 14. Changes of the V_v light-scattering pattern from a particular specimen PTMG(1000)–DMI:DAM with stretching, relaxing, and heat treatment in a highly stretched state.

propagating in the transverse direction to the stretching axis,[26] while the inclined streaks may be due to orientation crystallization of the soft segments similar to that found for natural rubber vulcanizates in highly stretched states.[27]

When comparing the scattering patterns, especially for the H_v polarization, of a highly stretched and relaxed specimen and of a highly stretched and heat-treated specimen with those which were merely stretched up to identical elongations, respectively, some interesting suggestions about the changes of the crystalline textures may be deduced. It seems reasonable to suggest that a considerable disintegration of the ordered texture and a recovery of the disintegrated crystalline textures are encountered with the treatments described above. However, the most significant suggestion must be based on the fact that every specimen has still a "four leaves" pattern characteristic of uniaxially deformed spherulitic crystalline texture irrespective of the degree of stretching and of the kinds of

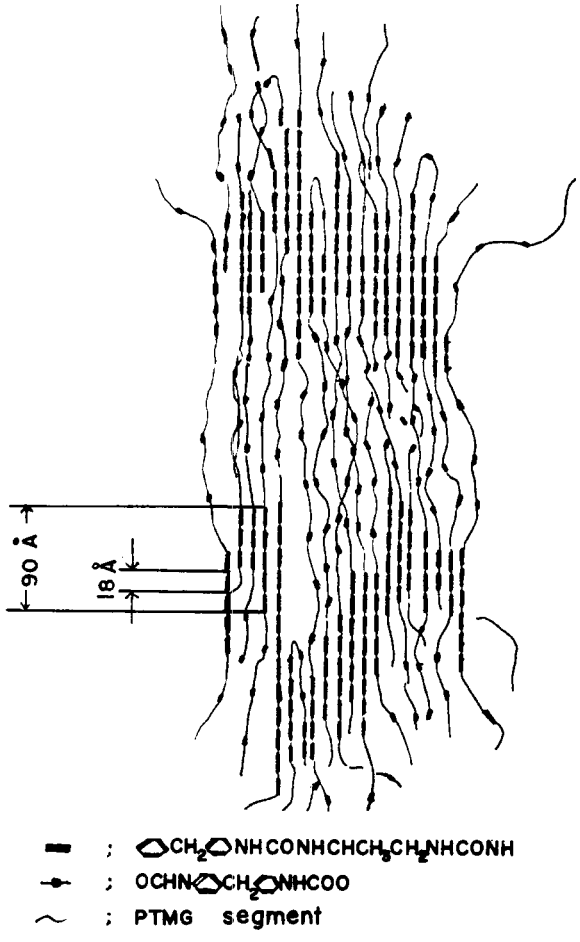

Figure 15. Schematic diagram illustrating a proposed model for the fiber structure of the segmented poly(urethaneureas) highly stretched and heat treated.

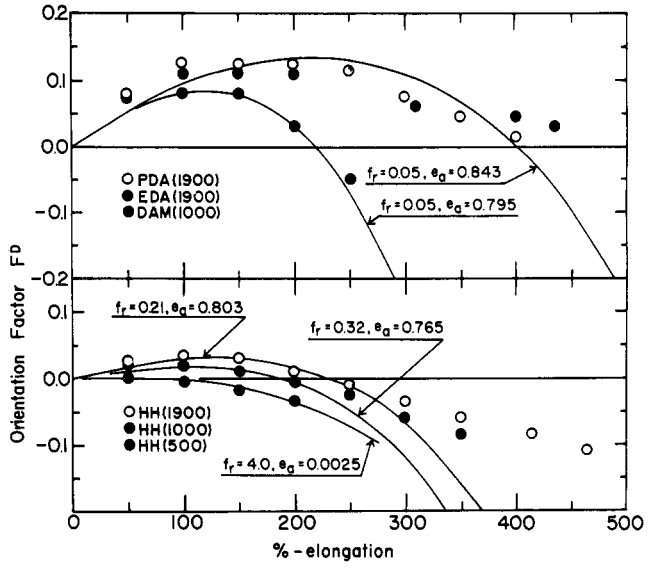

Figure 16. Comparison of observed results on the orientation behavior of transition moment of ν(C=O) with calculated ones based on a model of spherulite deformation, where the deformation parameters, J_B, f_C, J_C, l_C, m_C, n_C, and σ are fixed as 3.0, 0.5, 3.0, 1.0, 3.0, 1.0, and 2.0, respectively, but the other parameters f_r and e_a are chosen, as indicated in the figure, so as to give the best fit with the observed results at relatively small % elongations.

treatments it has received. That is, these results suggest that the crystalline textures are quite stable, being only slightly affected by the disintegration of the crystal lamella into less ordered crystalline fragments. This enables us to draw a schematic representation of the crystalline texture of highly stretched specimen, as illustrated in the right-hand side in Figure 10. Furthermore, it allows us to understand not only the transition of crystal orientation behavior but also the crystal orientation behavior during cyclic deformation shown in Figure 3. These can be understood in terms of greater or lesser orientation recovery of the crystalline textures themselves, in association with further reorientation of the fragmented crystallites within the disintegrated and disordered crystalline lamellae.

Figure 15 shows a proposed model for the fiber structure of the segmented poly(urethaneureas) heat treated in a highly stretched state, where the less ordered fragments of the lamella are realigned to the fiber axis to form an ordered structure, at least laterally. The model is mainly based on the chemical and wide-angle X-ray analyses. A rather localized structure is demonstrated by taking into account the good alignment of the hard segments to the fiber axis to remove the crystal defects caused by the orientation and disintegration of crystal lamellae; on the other hand, the highly deformed crystalline textures, as discussed above, are not taken into account.

Calculations of Crystal Orientation Based on a Model of Spherulite Deformation. Judging from the orientation behavior of the three crystallographic axes, especially the transition phenomena of orientation behavior of the transition moment of ν(C=O), and the existence of the spherulitic texture, the C=O bond and the chain axis must orient parallel and perpendicular to the radius of the spherulite, respectively. This behavior is similar to the orientation of the crystal b and c axes in a polyethylene spherulite. Thus, one can discuss the deformation mechanism of segmented poly(urethaneureas) more quantitatively in terms of the parameters of a spherulite deformation model proposed by some of the present authors for polyethylene.[28,29]

The deformation mechanism is divided into two steps.[29] The first step is an instantaneous orientation of the crystal lamellae in an affine fashion accompanied by twisting of the lamellae around their own axes due to straining of the tie-chain molecules, and is formulated for uniaxial deformation as

$$w'(\xi',0,\eta') = (w_0/8\pi^2)\{1 + \sigma(\lambda - 1)(1 - \xi'^2)\cos^2\eta'\} \times \lambda^3\{\lambda^3 - (\lambda^3 - 1)\xi'^2\}^{-3/2} \quad (2)$$

In this equation, w' is an orientation distribution function of the crystal lamellae within the spherulite in terms of three Euler angles with respect to the stretching direction, λ is the extension ratio of the spherulite, σ is a parameter representing easiness of the lamellar twisting, and W_0 is a normalization constant.

The second step is a delayed orientation of the fragmented crystallites forming a sort of mosaic structure within the crystal lamella, and is formulated by

$$q(\cos\beta,\alpha,\gamma) = (Q_0/8\pi^2)[f_r - f_C(\lambda - 1)\{R(\theta')/R_0\}^{J_C}P(\theta') + \{(1 - \cos^2\beta)\cos^2\alpha\sin^2\gamma\}^{J_B} + f_C(\lambda - 1)\{R(\theta')/R_0\}^{J_C} \times (\sin^4\theta' - \cos^4\beta + 2\cos^2\theta'\cos^2\beta)(e_a\cos^{2l_C}\alpha\sin^{2m_C}\gamma + e_r\cos^{2n_C}\alpha)] \quad (3)$$

Here q is an orientation distribution function of the crystallites within the crystal lamella in terms of three Euler angles with respect to the lamellar axis, and four types of orientations of the crystallites are taken into consideration. On the right-hand side of eq 3, the first term corresponds to the contribution from random orientation (type R) of the crystallites so that the parameter f_r is a measure

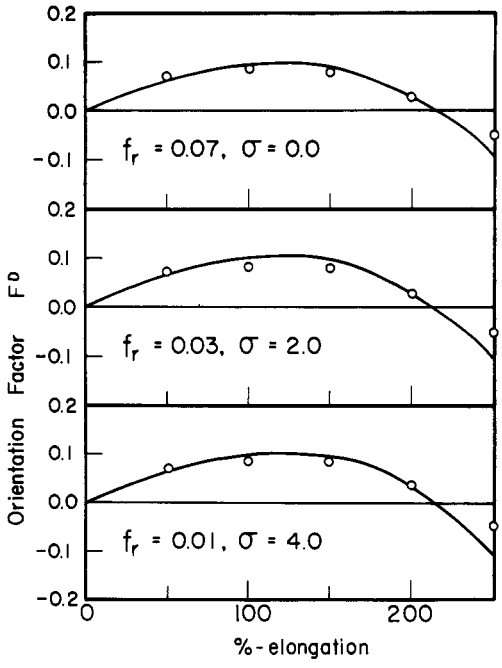

Figure 17. Comparison of observed results on the orientation behavior of transition moment of ν(C=O) with calculated ones based on a model of spherulite deformation, where the deformation parameters, J_B, f_C, J_C, e_a, l_C, m_C, and n_C are fixed as 3.0, 5.0, 3.0, 0.79, 1.0, 3.0, and 1.0, respectively, but the other parameters f_r and σ are varied so as to give the best fit with the observed results at relatively small % elongations.

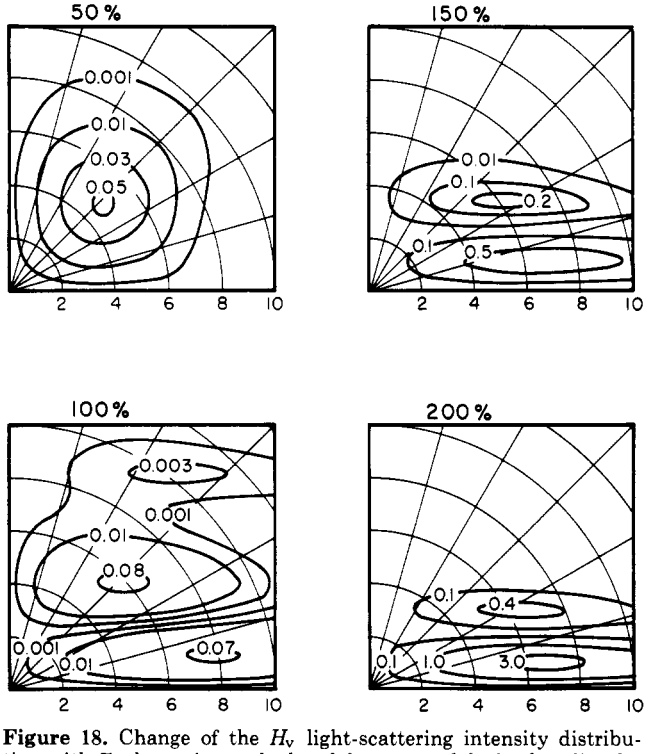

Figure 18. Change of the H_v light-scattering intensity distribution with % elongation, calculated from a model of spherulite deformation having the same deformation parameters as those in the upper part in Figure 17.

of the degree of imperfection of the lamella in the undeformed state. The second term is added in order to compensate for the variation of the constant Q_0 with polar angle θ', and the third term is the contribution from the crystallites with their C=O bond axes oriented parallel to the lamellar axis (type B) so that J_B is a parameter characterizing the sharpness of this type orientation distribution. The fourth term represents two types of orientations with the chain axis parallel to the stretching direction (types C_a and C_r), which arise from rotation of the crystallites around their own axes perpendicular to the plane including the C=O bond axis and chain axis, *i.e.*, from the reciprocal lattice vector of the M_1 plane, and from unfolding of the folded chain crystals, respectively. They are taken to differ in their effect as indicated by the insertion of the factors ($e_a \cos^{2l_C} \alpha \sin^{2m_C} \gamma$) and ($e_r \cos^{2n_C} \alpha$) in eq 3, where e_r is defined as ($1 - e_a$). In types C_a and C_r orientations, the parameters l_C, m_C, and n_C characterize the sharpness of the orientation distributions and the factor $[f_C(\lambda - 1)\{R(\theta')/R_0\}^{J_C}]$ indicates the dependence of the type C_a and C_r orientations on the extension ratios of the spherulite λ and of the crystal lamella $R(\theta')/R_0$ in terms of the parameters f_C and J_C.

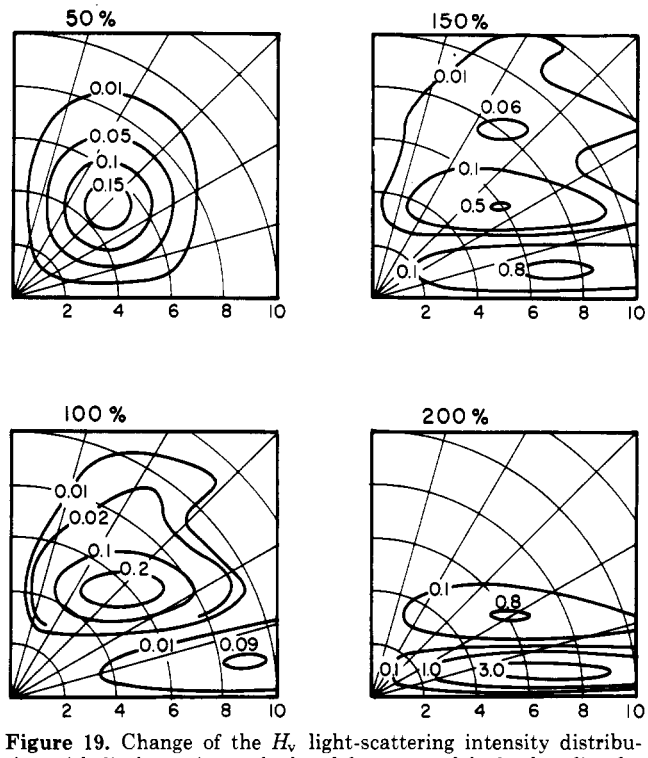

Figure 19. Change of the H_v light-scattering intensity distribution with % elongation, calculated from a model of spherulite deformation having the same deformation parameters as those in the middle part in Figure 17.

Figure 16 shows comparisons of the observed and calculated results on the orientation behavior of the transition moment ν(C=O). In the calculations based on the above model of spherulite deformation, the parameters, J_B, f_C, J_C, l_C, m_C, n_C, and σ are fixed as 3.0, 0.5, 3.0, 1.0, 3.0, 1.0, and 2.0, but the other parameters f_r and e_a are chosen so as to give the best fit with the observed results at relatively small elongations. Similar to Figure 11, PTMG(1000)-DMI:DAM, PTMG(1900)-DMI:PDA, and PTMG(1900)-DMI:EDA give a relatively well-defined four-leaf clover patterns of H_v light scattering, in contrast to PTMG(1900, 1000, 500)-DMI:HH, suggesting that the former three specimens have considerably well-developed spherulitic crystalline textures while the latter ones of the HH series do not. The facts that the orientation behavior of the former three specimens can be described, as seen in Figure 16, by using a relatively small value of f_r and a large value of e_a and *vice versa* for the latter specimens, are consistent with the above crystalline textures deduced from the light-scattering patterns. That is, the parameter f_r is a measure of the imperfection of the crystal lamella, and the parameter e_a and, in turn, the parameter e_r (= 1 − e_a) are the fractions of the transformed crystallites from

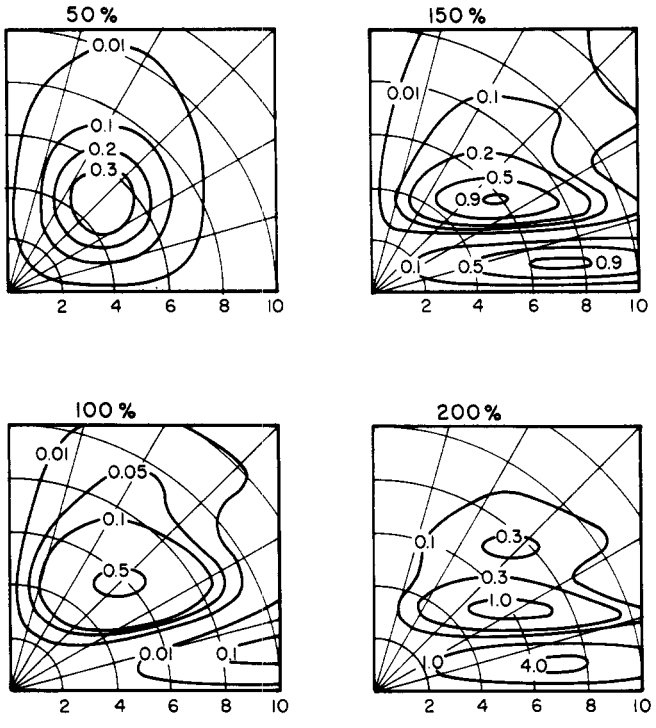

Figure 20. Change of the H_v light-scattering intensity distribution with % elongation, calculated from a model of spherulite deformation having the same deformation parameters as those in the lower part in Figure 17.

type B to type C_a (rotation of crystallite) and type C_r (unfolding). Thus, the larger the f_r and smaller the e_a, as is found in the case of PTMG(500)–DMI:HH, the less perfect are the crystal lamellae, if any, with respect to formation of a well-defined spherulitic texture, and are easily unfolded.

Figure 17 shows a similar comparison for PTMG(1000)–DMI:DAM by varying the values of f_r and σ but fixing the other parameters. As can be recognized from the results in the figure, a decrease of f_r has the same effect as an increase of σ upon the orientation behavior. Using these sets of the parameters, the intensity distribution of small-angle light scattering can be calculated under particular polarization conditions.[30] Figures 18–20 show the changes of the calculated H_v scattering patterns with uniaxial deformation of the spherulite. They give the lobes of the so-called four-leaf clover pattern in the initial stages of the deformation up to about 100% elongation. However, with a further increase of elongation, the lobes move to the zones near the equator and separate to produce the eight-leaf pattern.[18] In contrast to the above results on the counterbalanced effects of f_r and σ upon the orientation behavior of ν(C=O), the decrease of f_r increases the scattered intensity remarkably. This increase is probably due to an improvement of the orientation correlation of the scattering elements, while the increase of σ diffuses the scattered intensity mainly to the vertical direction.

Because only the crystalline orientations and not the noncrystalline ones were taken into account, the calculated results in Figures 18–20 differ considerably in detail from those observed in Figure 13. The elasticity of the segmented poly(urethaneureas) must be understood in terms of the orientation recovery of the soft segments, which is, however, more or less correlated with the deformation mechanism of the spherulitic crystalline textures discussed above.

Acknowledgments. The authors are indebted to the Toyo-bo Co., Ltd., for permission to publish this paper and to a grant from the Scientific Research Funds (Kagaku Kenkyu-hi, 743020-1972) of the Ministry of Education, Japan.

References and Notes

(1) (a) Presented at the 23rd International Congress of Pure and Applied Chemistry, July 29, 1971, Boston, Mass.; *Macromol. Prepr.*, **1**, 525; (b) From the Katata Research Institute, Toyo-bo Co., Ltd.; (c) from the Department of Polymer Chemistry, Kyoto University.
(2) (a) C. Sadron, *Angew. Chem.*, **75**, 472 (1963). (b) S. L. Aggarwal, Ed., "Block Copolymers," Plenum Press, New York, N. Y., 1970.
(3) G. E. Molau, Ed., "Colloidal and Morphological Behavior of Block and Graft Copolymers," Plenum Press, New York, N. Y., 1971.
(4) S. L. Cooper and A. V. Tobolsky, *J. Appl. Polym. Sci.*, **10**, 1837 (1968).
(5) S. B. Clough, N. S. Schneider, and A. O. King, *J. Macromol. Sci.-Phys., Part B*, **2**, 641 (1968).
(6) R. Bonart, *J. Macromol. Sci.-Phys., Part B*, **2**, 115 (1968); *ibid., Part B*, **3**, 337 (1969).
(7) H. Suzuki and H. Ono, *Bull. Chem. Soc. Jap.*, **43**, 682 (1970).
(8) H. Ishihara and I. Kimura, *Rept. Progr. Polym. Phys. Jap.*, **13**, 409 (1970).
(9) I. Kimura, H. Ishihara, K. Saito, and H. Ono, *Rept. Progr. Polym. Phys., Jap.*, **13**, 205 (1970).
(10) I. Kimura, H. Ishihara, K. Saito, K. Tamaki, and H. Ono, *Rept. Progr. Polym. Phys., Jap.*, **13**, 209 (1970).
(11) T. Uchida, T. Soen, T. Inoue, and H. Kawai, *J. Polym. Sci., Part A-2*, **10**, 101 (1972).
(12) T. Ono, H. Minamiguchi, T. Soen, and H. Kawai, *Kolloid-Z. Z. Polym.*, **250**, 394 (1972).
(13) L. L. Harrell, *Macromolecules*, **2**, 607 (1969).
(14) G. M. Estes, R. W. Seymour, and S. L. Cooper, *Macromolecules*, **4**, 452 (1971).
(15) S. Nomura, H. Kawai, I. Kimura, and M. Kagiyama, *J. Polym. Sci., Part A-2*, **5**, 479 (1967).
(16) T. Inoue, T. Soen, T. Hashimoto, and H. Kawai, *J. Polym. Sci., Part A-2*, **7**, 1283 (1969).
(17) E. Hirata, T. Ijitsu, T. Soen, T. Hashimoto, and H. Kawai, *Rept. Progr. Polym. Phys., Jap.*, **16**, 267 (1973); full paper will be submitted to *Polymer (London)*.
(18) M. Motegi, T. Oda, M. Moritani, and H. Kawai, *Polym. J. Jap.*, **1**, 209 (1970).
(19) S. Tatematsu, N. Hayashi, S. Nomura, and H. Kawai, *Polym. J. Jap.*, **3**, 488 (1972).
(20) M. Moritani, N. Hayashi, A. Utsuo, and H. Kawai, *Polym. J., Jap.*, **2**, 74 (1971).
(21) N. Hayashi, Y. Murakami, M. Moritani, T. Hashimoto, and H. Kawai, *Polym. J. Jap.*, **4**, 560 (1973).
(22) R. J. Samuels, *J. Polym. Sci., Part A-2*, **6**, 1101 (1968).
(23) R. J. Samuels, *J. Polym. Sci., Part A-2*, **9**, 2165 (1971).
(24) R. S. Stein and M. B. Rhodes, *J. Appl. Phys.*, **37**, 1873 (1960).
(25) R. J. Samuels, *J. Polym. Sci., Part C*, **13**, 37 (1966).
(26) T. Inoue, M. Moritani, T. Hashimoto, and H. Kawai, *Macromolecules*, **4**, 500 (1971).
(27) W. Yan and R. S. Stein, *J. Polym. Sci., Part A-2*, **6**, 1 (1968).
(28) S. Nomura, A. Asanuma, S. Suehiro, and H. Kawai, *J. Polym. Sci., Part A-2*, **9**, 1991 (1971).
(29) S. Nomura, M. Matsuo, and H. Kawai, *J. Polym. Sci., Polym. Phys.*, **10**, 2489 (1972).
(30) S. Nomura, M. Matsuo, and H. Kawai, submitted to *J. Polym. Sci., Polym. Phys. Ed.*